Hindawi
Geofluids
Volume 2019, Article ID 5723694, 16 pages
https://doi.org/10.1155/2019/5723694

Research Article

Numerical Simulation Study of Fines Migration Impacts on an Early Water Drainage Period in Undersaturated Coal Seam Gas Reservoirs

Xiaolong Peng,[1] Suyang Zhu ,[1] Zhenjiang You ,[2] Zhimin Du,[1] Peng Deng,[1] Chaowen Wang,[1] and Mingwei Wang[1]

[1]*State Key Laboratory of Oil and Gas Reservoir Geology and Exploitation, Southwest Petroleum University, Chengdu, China*
[2]*School of Chemical Engineering, The University of Queensland, Brisbane, Qld 4072, Australia*

Correspondence should be addressed to Suyang Zhu; suyang.zhu@swpu.edu.cn and Zhenjiang You; zhenjiang.you@gmail.com

Received 17 June 2019; Revised 28 October 2019; Accepted 4 December 2019; Published 30 December 2019

Academic Editor: Julien Bourdet

Coal fines migration exerts negative impacts on early water drainage of undersaturated coal seam gas (CSG) reservoirs. The complicated migration process results in ineffective and inaccurate forecast of coal fines production. Hence, a robust modelling tool is required to include the mechanisms of fines migration and to predict their impacts on rock and production. In this paper, fines migration in coal is categorized into three stages: generation, migration, and deposition processes. The corresponding models for different stages are established, including (1) a fines generation model, (2) the maximum fines-carrying concentration model and deviation factor of the modified Darcy model, (3) a fines deposition model, and (4) a dynamic permeability and porosity model. The above models are coupled with a water flow model, solved numerically using the finite difference method. Then, two dewatering strategies, including fast and moderate depressurization, are compared using the proposed models to study their effects on coal properties and following production. Finally, the production history of a CSG well in the Qinshui Basin, China, is utilized for history matching in a field case study. The simulation results indicate that new fines will be generated in a fast depressurization process and the water rate decline reduces the cleat permeability significantly. The newly generated fines can enhance the permeability temporarily, but they will block the flow channels and bring serious damage to the permeability when the water rate declines. The moderate depressurization strategy can produce the coal fines in a continuous mode, and the formation damage induced by fines deposition can be reduced to the acceptable level, which is the more reliable way to maintain well productivity. In addition, multiple well shut-in can trigger the irreversible fines deposition, reduce the permeability, and decrease the production rate.

1. Introduction

The dual porosity model is usually employed to describe the fluid flow in coal rock [1, 2]. In undersaturated CSG reservoirs, gas is stored in the matrix and the cleat (fracture) system is saturated with water [3, 4]. Owing to the undersaturated state of gas storage, water drainage is required to reduce pore pressure in coal. Then, gas in the matrix desorbs and subsequently flows through coal cleat system towards hydraulic fractures and then a wellbore or straight to a wellbore [5, 6]. For a saturated CSG reservoir, gas can be directly produced by a well and water drainage is not necessary. In the undersaturated CSG reservoirs, not only the fluids but also the transport of solid particles occurs in the coal cleats during the early water drainage period. Because of the high fragility, coal rock often generates large numbers of fines in drilling, stimulation, and water drainage processes [7–9].

During water drainage in CSG production, these pulverized coals (coal fines) continuously migrate in the cleat system and enter the wellbore accompanied by carrier water. As the water rate declines, coal fines may deposit in the cleat system and clog the flow channels in the coal seam [10, 11], reduce porosity and permeability [12, 13], hinder the water drainage, and decrease the productivity of CSG wells [14].

Furthermore, after coal fines enter the wellbore, these particles will block the pump and damage tubing pipes of the artificial lift facilities [15, 16]. Therefore, there exists a significant influence of fines migration on production of CSG reservoirs, and a practical model for coal fines migration in the cleat system is necessary for production analysis [17].

Fines produced from the CSG well are significantly different in particle size, micromorphology, mineralogy, and generation modes during different stages of production [18, 19]. Owing to the complexity of fines generation and migration, it is difficult to establish a robust mathematical model to evaluate the impacts of coal fines systematically and quantitatively. Traditionally, the study of fines migration in CSG reservoirs adopts the models on sand production in gas reservoirs [17, 20]. These models focus on fines production in sandstone reservoirs (sanding model) [21, 22] and can be employed to study the fines migration in CSG reservoirs. The sanding models are generally categorized as macro and micro models (network models). Macro models are established on the basis of continuous porous media, such as the models of Gruesbeck and Collins [23] and Ohen and Civan [24]. Network models describe the flow of fluid and solid particles from a microscopic perspective. However, assumptions and application conditions of fines migration in sanding models are significantly different from those in the coal seam. Three main differences in particle generation and migration processes exist between sandstone and coal seam, which include the following: (1) Particle shape in the sanding model is usually simplified as spherical. In contrast, the shape of coal fines is considerably complicated, particularly in planar, mesh, or needle-like shapes [25]. (2) The flow channels of sand grain and coal fines are quite different. The flowing paths for coal fines are a fracture-cleat system, and the paths for particles in sand are a pore-throat system of sandstone [26]. (3) Even if multiple simplifications are applied, the mathematical models for coal fines generation and migration are still too complicated to solve when these models are coupled with water and gas flow models. Therefore, a significant gap still exists between the available models and the robust model needed for actual fines production in CSG reservoirs.

In our previous study [27], the two-phase flow model is employed to study the flow of water and gas with coal fines, which provides a simple estimation of fines migration during the whole CSG production. However, the production history indicates that the primary stage of coal fines production is during the early water production of undersaturated CSG reservoirs [28, 29]. To focus on the coal fines migration in the early water drainage period, a series of models are proposed in this paper to study the migration of coal fines, including the generation, migration, and deposition processes and its impacts on coal properties. Based on these models and the mass conservation equation, a flow model is established to describe coal fines migration coupled with water flow. Then, three case studies and one field application are performed using a numerical simulation method to illustrate the mechanisms of coal fines migration and the effects of fines migration on coal properties and production rate.

The objective of this research is to develop the flow model of water and fines, study the law of coal fines flow, and explore the influence of coal fines migration on water production. This paper is organized as follows. Section 2 presents the conceptual models for coal fines migration in each flow stage. Section 3 describes the mathematical model for flow of water and coal fines. Section 4 investigates the impacts of coal fines migration on water production using three case studies and one field application.

2. Modeling on Coal Fines Migration

2.1. Conceptual Model. During the early production period of undersaturated CSG reservoirs, water is the only phase that flows in the coal and this provides the primary motivation for fines movement. Fines migration can be classified into three stages including generation, migration, and deposition, shown in Figure 1. Initially, all fines are in the static state. In the generation stage, when the water drainage begins, fines migrate with water owing to the flushing effect, which is the detachment process. If the water rate is higher than a critical value, the new fines will be generated from the surface of the coal cleat. This is the denudation process of coal fines. In the migration state, migration patterns include sliding on the pore surface, suspension, and rolling when fines flow. Models on sliding and rolling are very complicated, and the parameters in the models are inconvenient to obtain. Meanwhile, those models are difficult to couple with water flow. Hence, only the main pattern of fines flow, the suspension, is accounted for to simplify the migration stage in this study. In the deposition stage, as the water rate declines, coal fines may deposit in the cleat system, which is the reattachment process. The reattached fines can clog the flow channels, leading to the permeability damage, which is the blockage process.

Based on the physical process of coal fines migration, the entire flow process can be modeled using one curve (maximum water carrying capacity of coal fines), two states (static and flowing fines), three stages (generation, migration, and deposition), and four processes (detachment, denudation, reattachment, and blockage), shown in Figure 2.

Initially, all fines in coal are in the static state (Figure 2). When the water rate is higher than the critical value for flowing, coal fines begin to flow with the water phase. The migrating fines are in the flowing state. When the water rate is stabilized, the maximum mass of coal fines carried by water can be measured using laboratory tests. Inspired by the studies on the maximum retention function [30, 31], the curve generated in the present work is defined as the maximum water carrying capability of coal fines, which can be used to identify the state of fines. The maximum retention function focuses on the retention concentration of attached fines and its effects on porosity and permeability [32, 33]. The maximum water carrying capability concentrates on the start-up and flowing concentration of protogenetic fines and their state. These two functions are mathematically equivalent.

At state A shown in Figure 2, the point is above the curve, which indicates that a certain number of coal fines are in the flowing state and the other fines are in the static state.

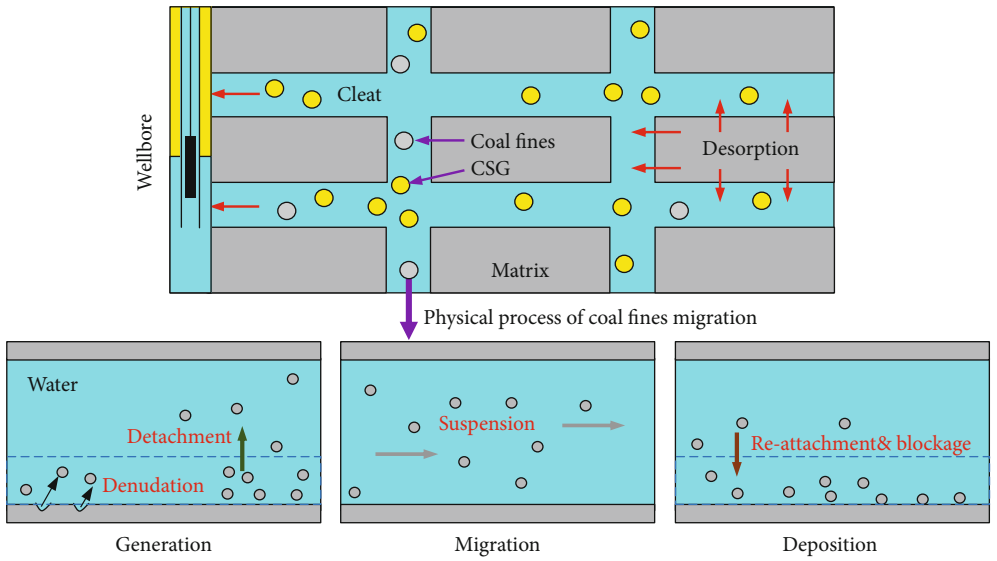

Figure 1: The flow stages and physical processes of coal fines during the production period.

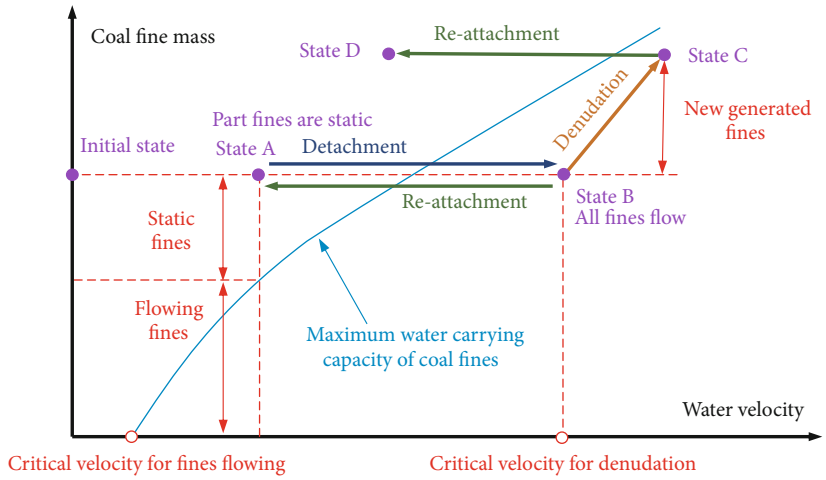

Figure 2: Schematic of the entire flow process of coal fines.

The transition from a static state to a flowing state is the detachment process.

As the water rate increases and the state moves to state B, the mass of fines is below the curve. This means that all fines are in the flowing state. If the state moves from states B to A, parts of flowing fines will deposit on the coal surface. The transition from a flowing state to a static state is named as the reattachment process of coal fines. When no new fines are generated (no denudation), the detachment and reattachment processes are reversible (Figure 2). Only static fines have a direct influence on coal permeability and porosity. Hence, the detachment and reattachment processes and the denudation process will directly and indirectly alter, respectively, the coal properties. When the water rate continues to increase and exceeds the critical velocity for denudation (states B to C in Figure 2), new fines will be generated owing to the water flushing effect. This is the denudation process of coal fines, which can increase the total mass of fines. The calculated denudation mass needs to be compared with the curve (the maximum water carrying capacity of coal fines) in Figure 2. If the mass of denudation corresponds to the point below the curve, the denuded fines are all in the flowing state. If the mass of denudation corresponds to the point above the curve (similar to state A), a certain number of coal fines are in the flowing state and the others are in the static state. When water production declines, the water velocity reduces and the state moves to point D. Since the fines mass is above the curve, the reattachment occurs and static fines increase. Note that the detachment and reattachment are irreversible when new fines are generated (denudation occurs).

To model the entire flow of coal fines (one curve, two states, three stages, and four processes), in the next section, the fines migration patterns will be analyzed and the migration model is established. Then, the generation and deposition models are constructed and finally the impacts of fines migration on coal properties are modeled.

2.2. Fines Migration Patterns. In this study, only the main pattern of fines suspension is accounted for to simplify the physical process. The mathematical model based on statistical regression will be in a simple form and beneficial for equation solving and parameter setting. Usually, the velocity, coal fines concentration, pressure, and fluid saturation are selected as the variables in the mathematical model, which is

$$C_f = C_f(\omega_w, p_w), \tag{1}$$

where C_f represents the coal fines concentration in water (g/ml). ω_w is the actual velocity of the water phase (cm/s). p_w is the water pressure (MPa).

The relationship between ω_w and the Darcy velocity v_w is as follows:

$$\omega_w = \frac{v_w}{\varphi}, \tag{2}$$

where φ represents the cleat porosity of coal (dimensionless). v_w is the Darcy velocity of the water phase (cm/s).

The pore pressure determines the deformation and state of fines, which affect the concentration of fines. When the elasticity of fines is noticeable, the deformation of particles cannot be neglected as pore pressure changes. In CSG reservoirs, the change of pore pressure varies from 4-6 MPa to 0.5-1 MPa and the state of fines (flowing and static) mainly depends on pressure difference, instead of pressure. Hence, the effect of pressure on the concentration of flowing fines can be neglected. So Equation (1) can be simplified as

$$C_f = C_f(\omega_w). \tag{3}$$

Therefore, the experimental method can be used to establish the relationship between the amount of coal fines and water velocity. The rest of these factors are integrated as parameters in the functional relations.

2.3. Modified Darcy Model for Water Flow with Coal Fines. Because the moving coal fines follow the water flow, the momentum equation of coal fines is the modified Darcy model. According to hydrodynamics, if there is no solid particle in the water, the water flow in the porous media obeys Darcy's law. While there are solid particles in the water stream, as the carrier medium, water will give kinetic energy to coal fines, leading to the velocity increase in fines and velocity decrease in water. Hence, the water velocity does not obey the standard Darcy's law in the flow of water and coal fines. The higher the concentration of coal fines, the more the kinetic energy exchange between water and coal fines. The concentration of coal fines is strongly dependent on the water velocity. However, most researchers ignored the effect of solid particles and applied the standard Darcy formula to approximate the water flow [34–36].

From the perspective of coal fines, the movement of solid particles in porous media is significantly different from that in a free stream. Hence, the flow model of water-coal fines in the coal cannot simply copy the water-sand flow model in the river (debris flow model) or particle flow model in the wellbore. There is one type of model that treats the particle and the carrier fluid velocity the same [23, 24, 34, 35]. This model cannot describe the phenomenon that the fluid is able to transport fines only if the velocity of water exceeds a certain minimum value [37]. For this reason, subsequent studies have introduced the velocity of fines (ω) and the critical water velocity. It suggests that fines will be static ($\omega = 0$) if the fluid velocity is below the critical velocity [38].

$$\omega = \begin{cases} 0, & (v_w < v_{sc}), \\ v_w, & (v_w \geq v_{sc}), \end{cases} \tag{4}$$

where ω is the velocity of coal fines (cm/s). v_{sc} is the critical velocity of the water phase to start the fines migration (cm/s).

However, the improvement still does not show the significant difference of velocity between fines and water. For instance, Zhao et al. obtained a group of data from laboratory tests, which reveals a linear relationship between the coal fines velocity and water velocity [37], written as

$$\omega = kv_w + v_{sc}, \tag{5}$$

where k is the coefficient of the regression relation (dimensionless).

In this paper, we establish the flow of water and coal fines movement models using the available experimental results. Note that both water velocity and the coal fines concentration are always changing with time, and they are very sensitive to the flow conditions; therefore, they can be treated as the two main variables in the equations of motion.

The coefficient of variation is used to describe the interferences between water and coal fines. This variable α is defined as the ratio of the water flow with coal fines divided by the flow velocity without fines, while the rest flow conditions are the same, which is

$$\alpha = \frac{v_w(C_f)}{v_w^0}, \tag{6}$$

where α is the deviation factor. v_w^0 is the water flow velocity without fines (cm/s).

v_w^0 can be expressed using Darcy's law, shown as

$$v_w^0 = -\frac{K}{\mu_w}\nabla(p_w + \rho_w g), \tag{7}$$

where ∇ is the Hamiltonian operator, K is the permeability of coal (mD). μ_w is the water viscosity (mPa·s). ρ_w is the water density (g/m^3). g is the gravity coefficient (9.8 N/kg).

The deviation factor α is associated with the concentration of fines and the velocity of the flow, shown as

$$\alpha = \alpha(\omega_w, C_f). \tag{8}$$

Then, we can revise the equation of water flow as

$$v_w = -\frac{\alpha K}{\mu_w}\nabla(p_w + \rho_w g). \tag{9}$$

The velocity of coal fines comes from the kinetic energy transfer of water, which implies that the velocity of fines depends on the velocity of water velocity. In addition, the concentration of fines also affects the flow of fines. Then, the velocity of coal fines ω is related to the water velocity and the coal fines concentration, which can be expressed as

$$\omega = \omega(v_w, C_f). \tag{10}$$

The function ω is determined by experiment. Those factors influencing the velocity of water and coal fines are considered parameters of this function. For example, β is defined as the ratio of the velocity of water to the coal fines velocity, written as

$$\omega = -\frac{\beta_1 \cdot K}{\mu_w}(\nabla p_w + \rho g) + \beta_2, \tag{11}$$

where β_1 and β_2 are the coefficients to be solved.

The force and flow conditions related to the coal fines are different in different directions; for example, there exists the gravity in the vertical direction. Different functions and different experiments are required to reflect the anisotropy of the water flow with fines. Note that the dimensionality of β_1 should be consistent with K and the dimensionality of β_2 needs to be consistent with ω.

2.4. Generation and Deposition of Coal Fines. The generation process of coal fines includes the detachment and denudation. The detachment means that the coal fines begin to flow when the water velocity is above the critical velocity. As the water velocity continues to increase, the denudation process occurs, which is the process that coal debris breaks from the surface of coal, leading to the generation of fines, as shown in Figures 1 and 2. According to the hydraulic dynamics, it is a challenge to create the precise translation model [12, 39]. Compared with the sedimentation of sand in the river and in the wellbore, transition is more complicated between the flowing state and static state of coal fines. It is not only related to the carrying capacity of water flow but also closely related to the porous space. As the velocity of the water is less than that required to carry fines, more coal fines will convert from the flowing state to the static state.

If the state transition model for solid particles is established using experimental results, the above challenges can be addressed [27, 39, 40]. Firstly, this paper employs the maximum concentration of fines carried by water to describe the migration and deposition patterns of fines. The maximum concentration relates to the velocity, flow regime (nonlinear or liner flow), viscosity of water, shape, and gravity of coal fines. For a given coal seam, the parameters of rock and fluids are specific and the maximum sand concentration that water can carry serves as a function of water velocity.

$$C_{mxf} = C_{mxf}(\omega_w), \tag{12}$$

where C_{mxf} is the monotonic function of the flow velocity (g/ml).

The higher the velocity, the larger the fines concentration. Then, the calculation of conversion from migration to deposition (stop of fines flow) is based on the transporting capability of water. When the flow velocity changes from v_w^1 to v_w^2, the conversion volume of coal fines M_{tr} would be

$$M_{tr} = C_{mxf}\left(v_w^2\right) - C_{mxf}\left(v_w^1\right). \tag{13}$$

As the water velocity increases, more coal fines will be transported by the water, and some deposited coal fines will be transited to movable ones. m_{tr} is the amount of conversion in unit time which is further defined as

$$m_{tr} = \frac{dM_{tr}}{dt} = \frac{C_{mxf}\left(v_w^2\right) - C_{mxf}\left(v_w^1\right)}{\Delta t} = \frac{\partial C_{mxf}}{\partial v_w}\frac{\partial v_w}{\partial t}, \tag{14}$$

where m_{tr} is the amount of conversion per unit time and unit volume (transition velocity) (g/ml·s), d is the differential operator, Δt is the time difference (s), and ∂ is the partial derivative operator.

The conversion is not only influenced by transporting capacity of water but also restricted by the concentration of flowing coal fines and static coal fines (C_f and C_s). As the coal fines convert from the deposition state to the migration state, the amount of the conversion should not exceed the amount of static coal fines. When migrating coal fines come to the deposition state, the conversion amount should be less than the amount of the migration coal fines in the water. Hence, Equation (15) needs to be further restricted:

$$m_{tr} = \begin{cases} \dfrac{\partial C_{mxf}}{\partial v_w}\dfrac{\partial v_w}{\partial t}, & \text{if}\left(\dfrac{\partial v_w}{\partial t} > 0, C_s > 0\right)\text{or}\left(\dfrac{\partial v_w}{\partial t} < 0, C_f > 0\right), \\ 0, & (\text{else}). \end{cases} \tag{15}$$

When the water velocity continues to increase, new coal fines will be denuded from the surface of the cleat. To describe the effects of denudation on coal properties and coal fines volume, the total denudation of coal fines and the amount of conversion per unit time (denudation velocity) are employed. Their relation can be described as follows:

$$M_{pr} = \int_{t^{i-1}}^{t^i} m_{pr}\,dt, \tag{16}$$

where M_{pr} is the total denudation of coal fines during the time of t^{i-1}~t^i (g/ml). m_{pr} is the amount of denudation in unit time (g/ml·s).

When the water production rate declines, the coal fines deposit and clog the flow channels. If the agglomeration of

coal fines does not occur, the deposition (reattachment) shares the same critical velocity condition with the detachment, as shown in Equation (4). When the water velocity is above the critical value, the detachment occurs. When water velocity is below the critical value, the reattachment process happens.

2.5. The Impact of Coal Fines Migration on Porosity and Permeability of Coal. Fines denudation, detachment, and reattachment of coal fines generally cause changes of porosity and permeability of coal. Firstly, if fines get off from rock skeleton (denudation), a pore space and porosity of coal increase. Secondly, because the static fines occupy part of the pore space, the volume of the water will decline. Thirdly, the reduction of porosity due to deposition of coal fines is equal to the sum of the denudation volumes of the coal fines, which is expressed in Equation (17a). The permeability model of coal can be employed to describe the permeability damage induced by porosity [41–44], shown in Equation (17b):

$$\phi = \phi_{\mathrm{i}} + \sum_{i=0}^{i=n} \frac{M_{\mathrm{pr}}^{i}}{\rho_{\mathrm{s}}}, \tag{17a}$$

$$k = k_{\mathrm{i}} \left(\frac{\phi}{\phi_{\mathrm{i}}}\right)^{3}, \tag{17b}$$

where ϕ_{i} is the initial porosity, k_{i} is the initial permeability (mD), and ρ_{s} is the density of coal fines (g/ml).

3. Coupling Flow Model of Water and Coal Fines

3.1. Mathematical Model of Coupling Flow. Based on the conventional flow model and the models for fines generation, migration, deposition, and plugging, which are established in Section 2, the mathematical model of water flow can be coupled with coal fines models. In this study, we focus on fines migration and its impacts on coal properties during the early water drainage period. The assumptions are listed as follows.

(1) Coal seam is described by a dual porous medium consisting of a coal matrix and cleat system. Water and fines can only flow in cleats but not in a matrix

(2) The fluid flow in cleats is laminar (Darcy flow) under isothermal condition

(3) The coal fines are divided into static coal fines (deposition state) and flowing coal fines (migration state). The transition time between these two states is negligible

(4) The gas content in the matrix is set to zero. Only water production with fines migration is discussed

(5) The agglomeration of coal fines does not occur

According to the mass conservation, differential equations of the flow model are established for water and coal fines, respectively.

(1) *Water Flow.*

$$\nabla \cdot (\rho_{\mathrm{w}} v_{\mathrm{w}}) + \frac{\partial(\rho_{\mathrm{w}}\phi)}{\partial t} = q_{\mathrm{w}}. \tag{18}$$

Substituting the water velocity in Equation (9) into Equation (18) gives

$$-\nabla \cdot \left[\frac{\alpha K}{B_{\mathrm{w}}\mu_{\mathrm{w}}}(\nabla p_{\mathrm{w}} + \rho_{\mathrm{w}} g)\right] + \frac{\partial}{\partial t}\left(\frac{\phi}{B_{\mathrm{w}}}\right) = \frac{q_{\mathrm{w}}}{Z_{\mathrm{w}}}. \tag{19}$$

Equation (19) considers the influence of coal fines and brings in deviation coefficient α, which is a function of the flow velocity and the concentration of movable coal fines. q_{w} is the source-sink term of water (m^3/ks) (ks = kilo second).

(2) *Mass Conservation of Flowing Fines in Water.*

The mass conservation equation for migrating coal fines is

$$\nabla \cdot (\rho_{\mathrm{s}}\omega) + \frac{\partial(\rho_{\mathrm{s}} C_{\mathrm{f}}\phi)}{\partial t} = -\left(m_{\mathrm{tr}} + m_{\mathrm{pr}}\right)\rho_{\mathrm{s}}. \tag{20}$$

Differentiating both sides of Equation (10), Equation (21) can be derived as follows:

$$\nabla \cdot \omega = \frac{\partial \omega}{\partial \omega_{\mathrm{w}}}\nabla \omega_{\mathrm{w}} + \frac{\partial \omega}{\partial C_{\mathrm{f}}}\nabla C_{\mathrm{f}}, \tag{21}$$

$$c_{\mathrm{s}}(\omega \cdot \nabla P) + \frac{\partial \omega}{\partial \omega_{\mathrm{w}}}\nabla \cdot \omega_{\mathrm{w}} + \frac{\partial \omega}{\partial C_{\mathrm{f}}} \cdot \nabla C_{\mathrm{f}} + \frac{\phi}{\rho_{\mathrm{s}}}\frac{\partial C_{\mathrm{f}}}{\partial t} + 2c_{\mathrm{s}}\phi\frac{\partial p_{\mathrm{w}}}{\partial t} = -\frac{m_{\mathrm{tr}}}{\rho_{\mathrm{s}}} - \frac{m_{\mathrm{pr}}}{\rho_{\mathrm{s}}}. \tag{22}$$

Because the coal is slight compressible, the compressibility coefficient c_{s} is a very small value. Therefore, we can further simplify Equation (22) as

$$\frac{\partial \omega}{\partial \omega_{\mathrm{w}}}\nabla \cdot \omega_{\mathrm{w}} + \frac{\partial \omega}{\partial C_{\mathrm{f}}}\nabla \cdot C_f + \frac{\phi}{\rho_{\mathrm{s}}}\frac{\partial C_{\mathrm{f}}}{\partial t} + 2c_{\mathrm{s}}\phi\frac{\partial p_{\mathrm{w}}}{\partial t} = -\frac{m_{\mathrm{tr}}}{\rho_{\mathrm{s}}} - \frac{m_{\mathrm{pr}}}{\rho_{\mathrm{s}}}. \tag{23}$$

Substituting Equation (2) and Equation (9) into Equation (23), we obtain

$$-\frac{\partial \omega}{\partial \bar{\omega}_{\mathrm{w}}}\nabla \cdot \frac{K}{\phi\mu_{\mathrm{w}}B_{\mathrm{w}}}[\nabla p_{\mathrm{w}} + \rho_{\mathrm{w}} g] + \frac{\partial \omega}{\partial C_{\mathrm{f}}} \cdot \nabla C_{\mathrm{f}} + \left(\frac{\phi}{\rho_{\mathrm{s}}}\frac{\partial C_{\mathrm{f}}}{\partial t} + 2c_{\mathrm{s}}\phi\frac{\partial P_{\mathrm{w}}}{\partial t}\right) = -\frac{m_{\mathrm{tr}}}{\rho_{\mathrm{s}}} - \frac{m_{\mathrm{pr}}}{\rho_{\mathrm{s}}}. \tag{24}$$

(3) *Mass Conservation of Static Fines.*

$$\frac{\partial(\rho_{\mathrm{s}} C_{\mathrm{s}}\phi)}{\partial t} = m_{\mathrm{tr}}, \tag{25}$$

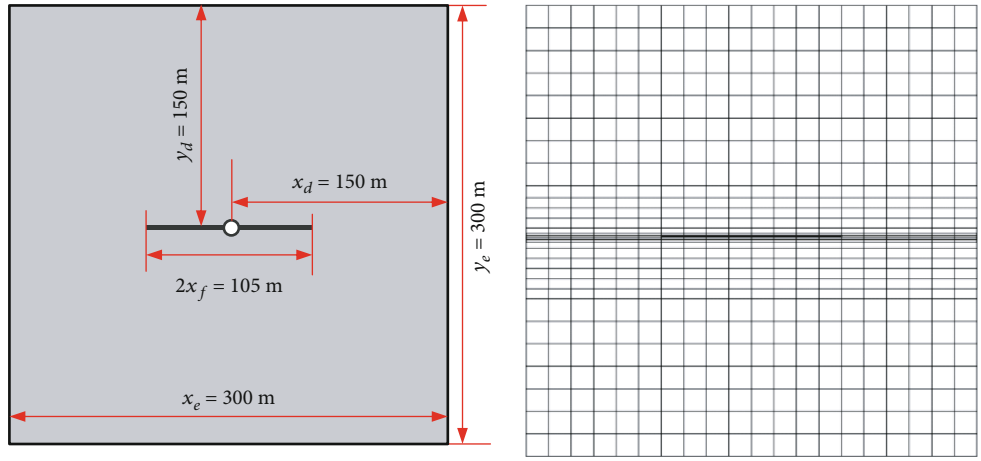

(a) The computational model (b) The grid system

FIGURE 3: The scheme of the simulation case.

where C_s is the concentration of static fines in the coal cleat (g/ml).

The variation of static fines concentration depends on the conversion between migration and settling. In order to solve the above governing equations, the definite conditions of the partial differential equations are also given, including the boundary and initial conditions. The boundary conditions include the inner boundary conditions (Γ_w) and the outer boundary conditions (Γ_r), which represent the production constraint and reservoir boundary, respectively. The inner boundary condition for pressure is

$$p|_{\Gamma_w} = p_w. \tag{26}$$

Outer boundary conditions are close boundary (constant flow rate). The constant flow boundary is also called the second boundary condition. In the flow model of CSG, the outer boundary condition is usually the closed boundary, which means that there is no flowing on the external boundary. It is written in the form

$$\frac{\partial p(x,y,z,t)}{\partial n}|_{\Gamma_r} = 0, \tag{27}$$

where n represents the normal direction.

The initial conditions of the model are the given initial pressure, fluid saturations, and gas content distribution.

$$p(x,y,z,t)|_{t=0} = p_0(x,y,z,0), \tag{28}$$

$$C_s(x,y,z,t)|_{t=0} = C_{s0}(x,y,z,0), \tag{29}$$

$$C_f(x,y,z,t)|_{t=0} = C_{f0}(x,y,z,0). \tag{30}$$

Due to the complexity of the model, numerical simulation is applied to solving the governing equations. The detailed numerical solution of this model is provided in the appendix.

3.2. Simulation Settings. A computational model in Figure 3(a) is employed for numerical analysis of fines migration during the early water drainage period. The radius of the wellbore is 0.06 m, and the size of the simulation domain is 300 m × 300 m × 5 m. The depth of the CSG reservoir is 400 m from the surface. The external boundary is specified as no-flow boundary, and the internal boundary is the constant water production rate. In this study, an important assumption is that the coal fines in the wellbore can be produced immediately and do not affect the efficiency of pump and water production. The local refined orthogonal grid system is used to represent the hydraulic fracture of the well (Figure 3(b)).

The cross-sectional area of the simulation grid for hydraulic fracture is 5 m × 1.25 m. The fracture permeability owns finite conductivity, which is 15 mD. Fracture half-length is 52.5 m. Initially, 5% of static coal fines are in the cleat system. The other parameters are listed in Table 1.

The model parameters in Sections 2.1 and 2.2 need to be obtained from experimental data, which is hardly available in the literature. In the present study, these parameters are assumed based on limited literatures [27], which are shown in Tables 2 and 3.

The relative permeability and capability pressure curves can be obtained from our previous study [27], shown in Figure 4.

The mass of maximum carrying fines can be calculated as the product of m_{tr}, volume of grid V_{grid}, porosity ϕ, and the time interval Δt, as shown in Equation (31). The mass of denudation fines can be calculated as the product of m_{pr}, V_{grid}, ϕ, and Δt, as shown in Equation (32).

$$m_{carry} = m_{tr} V_{grid} \phi \Delta t, \tag{31}$$

$$m_{denudation} = m_{pr} V_{grid} \phi \Delta t, \tag{32}$$

where m_{carry} is the mass of maximum carrying fines (mg), $m_{denudation}$ is the mass of denudation fines (mg), V_{grid} is the

Table 1: Basic parameters of the model.

Parameter	Value
Initial concentration of static fines (%)	5
Initial concentration of flowing fines (%)	0
Initial water saturation (%)	100
Fracture height (m)	5
Porosity of cleat (dimensionless)	0.008
Permeability of cleat (mD)	1
Porosity of hydraulic fracture (dimensionless)	0.05
Permeability of hydraulic fracture (mD)	20
Grid size on the x direction	15
Grid size on the y direction	15, 7.5, 1.25
Grid size on the z direction	5
Initial pressure of coal (MPa)	4
Compressibility of coal (10^{-4} MPa^{-1})	2.354
Water density (g/cm^3)	1.08
Coal fines density (g/cm^3)	1.38
Water dynamic viscosity (mPa·s)	1

Table 2: The assumed deviation factor of water velocity response to pure water velocity and coal fines concentration.

ω	1.14	1.04	0.762	0.424	0.411	0.134	0
v_w	0.9	0.8	0.6	0.4	0.2	0.1	0
C_f	0.05	0.01	0.02	0.05	0.06	0.08	0.1

Table 3: Assumed water velocity deviation factor.

α	0.912	0.863	0.741	0.711	0.531	0.314	0
v_w	0.9	0.8	0.6	0.4	0.2	0.1	0
C_f	0.05	0.01	0.02	0.05	0.06	0.08	0.1

volume of the simulation grid (cm^3), and Δt is the time interval (s). The obtained water carrying capacity of coal fines (m_{carry}) and the denudation mass ($m_{denudation}$) as functions of water velocity are presented in Figures 5(a) and 5(b), respectively.

4. Result and Discussion

4.1. Case 1: Coal Fines Concentration under Two Dewatering Strategies. Case 1 compares coal fines transport under moderate and fast depressurization strategies. The moderate depressurization adopts a relatively low initial water rate, which is often deployed in stress-sensitive coals. The fast depressurization strategy implies a higher initial water rate. This is a common production strategy to fast decrease the pore pressure and lead to better gas production in undersaturated CSG reservoirs.

Figure 6 shows that the coal fines concentration curves in 10 grids from the wellbore side (near to the wellbore) to the edge side (far from the wellbore) when the water rate is set as 6 m^3/day (moderate depressurization strategy). Grid 1 is the first grid, and grid 10 is the tenth grid away from the wellbore in the y direction.

The decrease in static fines concentration and increase in flowing fines concentration demonstrate the phenomenon that coal fines can continuously move from the reservoir to the wellbore (Figures 6(a) and 6(b)). The flowing fines concentration is lower than the static fines concentration, which means that no new fines are generated (no denudation) when the moderate depressurization strategy is employed to dewater the coal.

When no denudation occurs, the static fines are carried by water with an extremely low concentration (almost zero) in the grid (Figure 6(a)). As the production proceeds, the static fines concentration decreases and the flowing fines concentration increases from grid 1 to grid 10. This indicates that the fines detach and migrate in the coal. Meanwhile, the highest concentration of flowing fines is slightly lower than the initial static fines concentration (Figure 6(b)). This results from fines production and porosity change induced by static fines concentration. It provides the fines distribution when no new fines are generated. Hence, the moderate depressurization strategy can assist the fines production and would not generate new fines, which can contribute to the appropriate fines production.

As the water production rate raises to 12 m^3/day, the static fines concentration will not reduce to 0 (Figure 7(a)) and the concentration of flowing fines (Figure 7(b)) is much higher than that of the initial static fines owing to the denudation effect (Figure 7(c)). The mass of denuded fines is directly obtained using the relationship in Figure 5(b). The results indicate that the static fines cannot be completely removed by water flow at the same velocity (Figure 7(a)). Figure 7(b) indicates that the concentration of flowing fines is continuously increasing from grid 10 to 1, because fines from other parts of coal have accumulated near the wellbore. When new fines are generated in the grid (Figure 7(c)), it leads to a lower decreasing rate of static fines concentration (comparing Figures 6(a) and 7(a)) and a higher increasing rate of flowing fines concentration (comparing Figures 6(b) and 7(b)).

Case 1 illustrates the fines migration in coal with and without a denudation effect when the water production remains at a constant rate. In an undersaturated CSG reservoir, the water rate will decline as the gas desorption begins and always changes during the early drainage period. Therefore, the effects of various water rates on fines migration are analyzed in Case 2 in the next section.

4.2. Case 2: The Effect of Water Rate Variation. The main purpose of Case 2 is to study the influence of water rate change on fines deposition and migration in coal. At the beginning, the initial water production rate of four schedules is set as 12 m^3/day for the first 20 days to start the fines migration and denudation. Then, for the following 20 days, the water rate of schedule 1 remains 12 m^3/day and water rates are set as 6, 2, and 0 m^3/day for schedules 2-4, respectively. Figure 8(a)

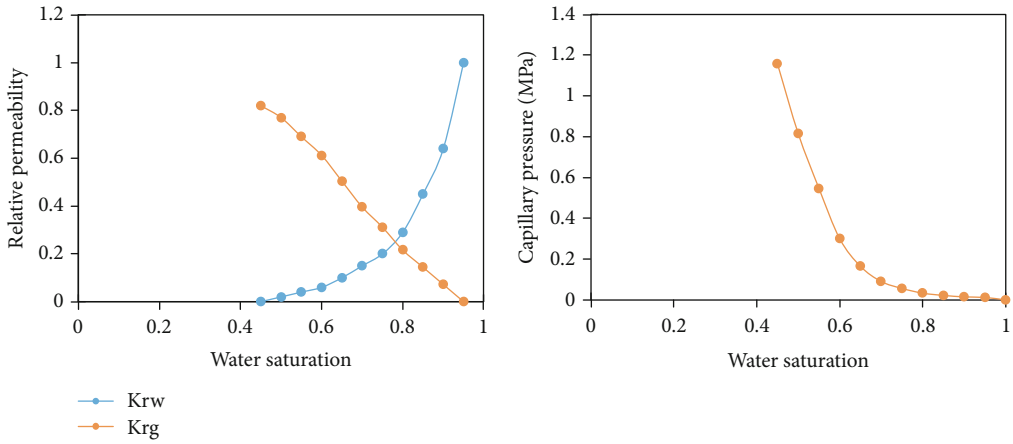

(a) Relative permeability (b) Capillary pressure

Figure 4: The relative permeability and capillary pressure of coal.

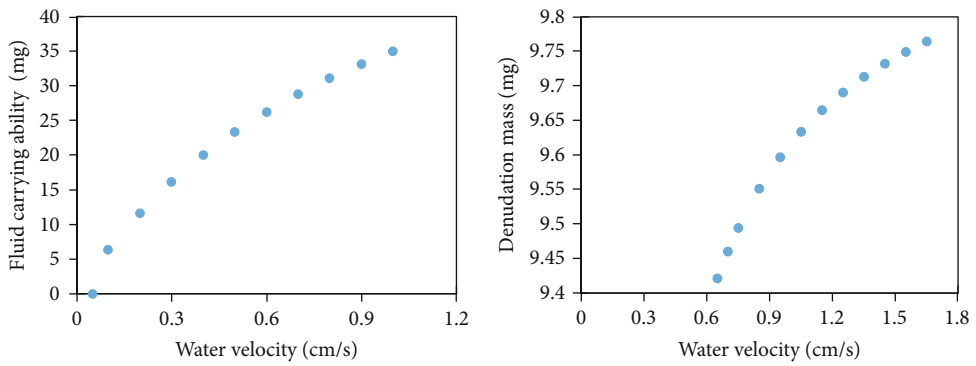

(a) The water carrying capability of coal fines (b) The mass of denudation fines

Figure 5: The assumptions on calculation parameters.

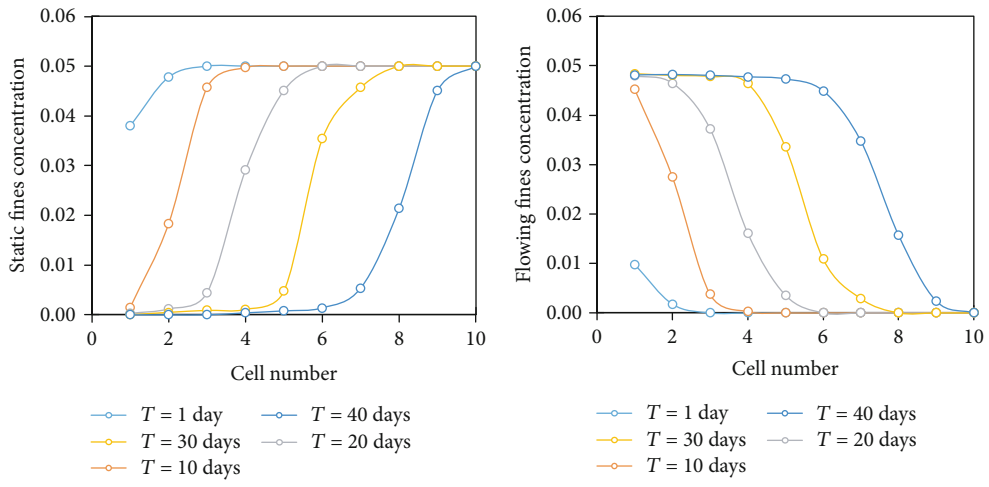

(a) Static fines concentration (b) Flowing fines concentration

Figure 6: Profile of coal fines in the reservoir at 6 m^3/day.

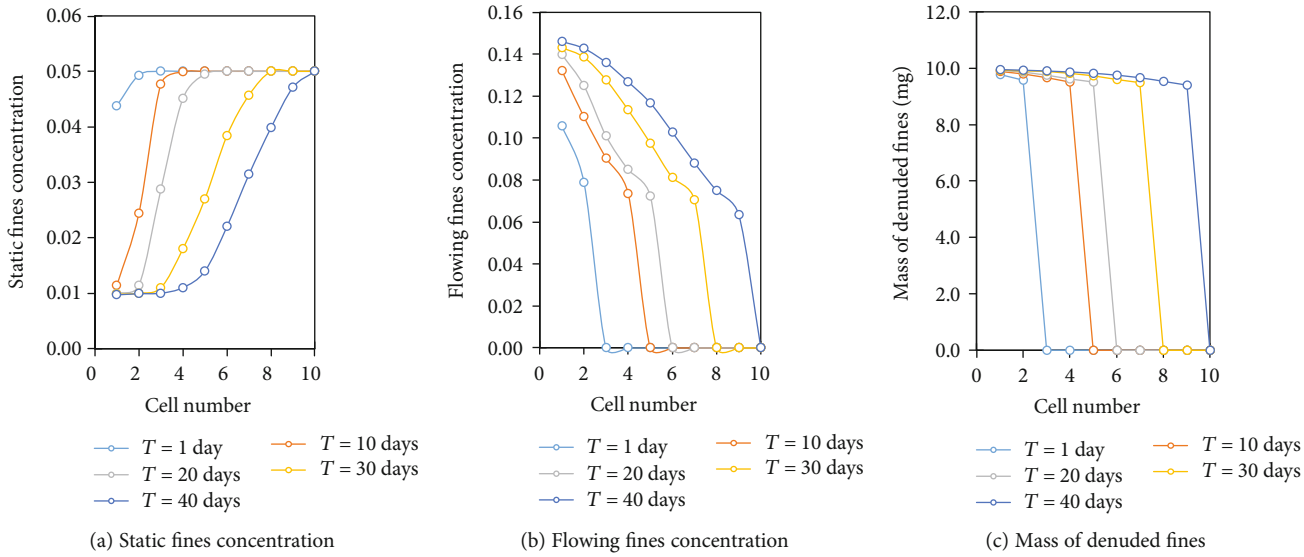

(a) Static fines concentration (b) Flowing fines concentration (c) Mass of denuded fines

Figure 7: Profiles of coal fines in the reservoir at 12 m^3/day.

shows static coal fines concentration profiles in 10 grids for the four schedules at 1 day after the well production rate has been changed ($T = 21$ days). It is shown that the water drainage rate has an important influence on the concentration of coal fines.

In schedule 1, the fines concentration is similar to that shown in Figure 7. Although new fines are generated in schedule 1, the constant water flow can continuously carry fines, leading to a low concentration of static fines. In schedules 2-4, coal fines deposition occurs near the wellbore owing to the abrupt decrease in the water rate. The deposition contributes to the dramatic increase in static fines concentration.

After well shut-in (schedule 4), the flowing fines concentration in grid 1 decreases from 0.1420 to 0.0524 in one day (Figure 7(b)), leading to the increase in static fines concentration from 0.0097 to 0.1040 (Figure 7(a)). The increase in static fines concentration is higher than the decrease in flowing fines concentration because the flow fines in grid 2 also migrate to grid 1 and increase the static fines concentration. This indicates that fines can easily accumulate near the wellbore and the blockage near the wellbore is much more serious than that away from the wellbore.

With reference to the concentration of static fines in Figure 8(a), the permeabilities of grids in the hydraulic fracture are presented in Figure 9 under different schedules. With the constant water drainage rate, the coal fines move to the wellbore along the water flow path. The accumulation of the coal fines will not occur because of the continuous water flow (the permeability profile under water schedule 1 in Figure 9). The water rate decrease can cause the fines deposition. The fines transport in cleats requires a continuous water flow and an appropriate water schedule. Both Figures 8 and 9 show the effects of well shut-in on the fines migration and coal properties.

During the early drainage period of CSG reservoirs, well shut-in often occurs due to the pump accident induced by fines production. The water production performance always has a significant change after multiple well shut-in. The impacts of multiple well shut-in on coal permeability are investigated in Case 3 in the next section.

4.3. Case 3: The Effect of Multiple Well Shut-in. This case is to study the influence of the multiple well shuts on permeability. The dewatering schedule is set as 4 cycles. In each cycle, the water rate is 15 m^3/day for 6 days and zero for the following 4 days. Two simulations are run with and without considering the coal fines migration process (Figure 10(a)).

Figure 10(a) shows that the water rate is the same in each cycle when coal fines migration is not included in the simulation. This is because the coal permeability does not change without the effects of fines migration. Considering the coal fines migration, the water rate cannot remain 15 m^3/day at the beginning of the second circle. This is because the fines deposition occurs when the well is shut. When the dewatering process goes in the second circle, the fines begin migrating and the coal permeability is enhanced. This leads to the recovery of water rate but still cannot return to 15 m^3/day in the second cycle. During the third and fourth circle, the peak water rates decline, which indicates that the flow channels have been clogged due to multiple well shuts.

Figure 10(b) indicates the permeability of different grids in the simulation considering fines migration. The permeability far from the wellbore (grids 7 and 10) continuously increases, because the concentration of static fines decreases and denudation does not occur owing to the low water rate. The permeability near the wellbore (grids 1 and 3) decreases after the well shut. This results from the fact that new fines are generated and participate in the flow because of higher water flux in the grid nearer to the wellbore. When the well is shut, new generated fines and flowing fines deposit and clog the flow channels in the coal seam. Although the permeability far from the wellbore increases, the permeability variation near the wellbore has a dramatic influence on well productivity.

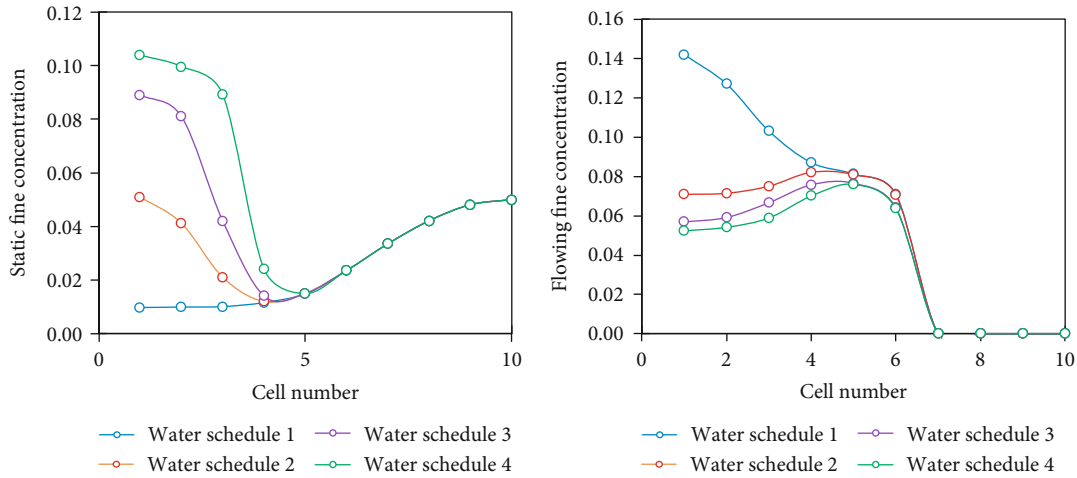

(a) Static fines concentration

(b) Flowing fines concentration

Figure 8: Profiles of coal fines under different water schedules.

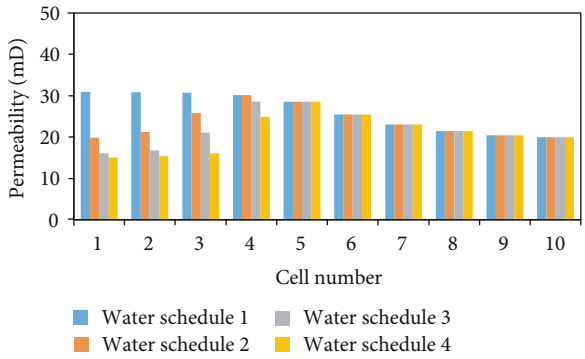

Figure 9: Permeability profiles under different schedules.

The simulation studies indicate that when the water rate is too high, new generated fines can clog the flow channels as water production changes. Multiple well shutting would dramatically decrease the well productivity owing to fines migration problem. If the impacts of fines migration are ignored in the simulation, an unreasonable dewatering strategy may be drawn for a specific CSG reservoir. For instance, results from the commercial simulator show that the higher the water rate, the higher the gas production rate, which is in contradiction with field observation [27].

4.4. Field Case Study. A field case is applied using a CSG well from the southern part of the Qinshui Basin, China. This well is named as ZY-n and extracts gas from coal seam #3, which has the largest gas reserve in the Qinshui Basin. The rank of coal seam #3 is high, and the gas content ranges from 8 to 21 m^3/t in an unsaturated sorption state. Hence, the dewatering is required to reduce the pore pressure.

The production history of the well ZY-n is shown in Figure 11. The initial dewatering rate was set as approximately 5 m^3/day. Then, the water rate increased to 9 m^3/day to shorten the drainage period. As the gas production began, the fast depressurization strategy is deployed (water rate = 10 m^3/day) to decrease the pore pressure fast. This treatment generated more coal fines, leading to a rapid decline of both water and gas production. The well ZY-n was shut for 9 times because of pump accidents caused by fines production. Consequently, the permeability of coal had been seriously damaged and this well was producing with low efficiency.

During the first 280 days (before gas production), this well was shut 6 times and the last 5 times were because of pump accidents owing to fines migration (Figure 11(b)). According to the log of production, well washing work had to be conducted to clean the fines in the wellbore. For the first well shut, the false data exists in the pressure profile since it was a constant value. For the second to fourth well shuts, the bottomhole pressure could not recover quickly, and the pressure even declined during the fifth and sixth well shuts (Figure 11(b)). Therefore, the early drainage period of the well ZY-n is selected for the field case study.

Because the stratigraphical dip angle is very small for coal seam #3 (approximately 3 degrees) and coal thickness does not vary for the well ZY-n, the numerical model in this paper can be employed to perform the history matching of the well ZY-n. The orthogonal grid system is chosen to simulate the water production. The outer boundary is set as the closed boundary condition, which means that the flux through boundary is zero. The production constraint is the bottomhole pressure, which is the internal boundary of the mathematical model. The water rate is the matching target in this case. The simulation parameters for history matching of the well ZY-n are listed in Table 4. Other simulation settings are the same as those in Section 3.2.

In history matching, the bottomhole pressure is the input parameter for production constraint and the water rate is the output parameter for matching. During history matching, the reservoir parameters of the abovementioned CSG well are adjusted, which are listed in Table 4.

Since the exact mass of produced fines was not recorded, the volume of fines can be only judged using the record of the color of drainage water and the history matching has to be proceeded qualitatively (dark blue line in Figure 12). After matching the production history, the static fines concentration and

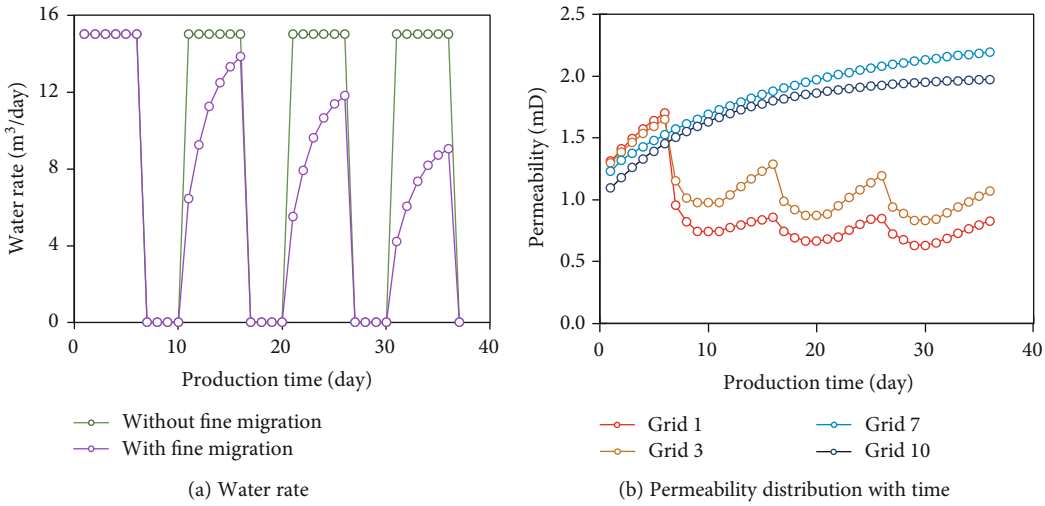

(a) Water rate (b) Permeability distribution with time

Figure 10: The effect of multiple well shut on early water drainage.

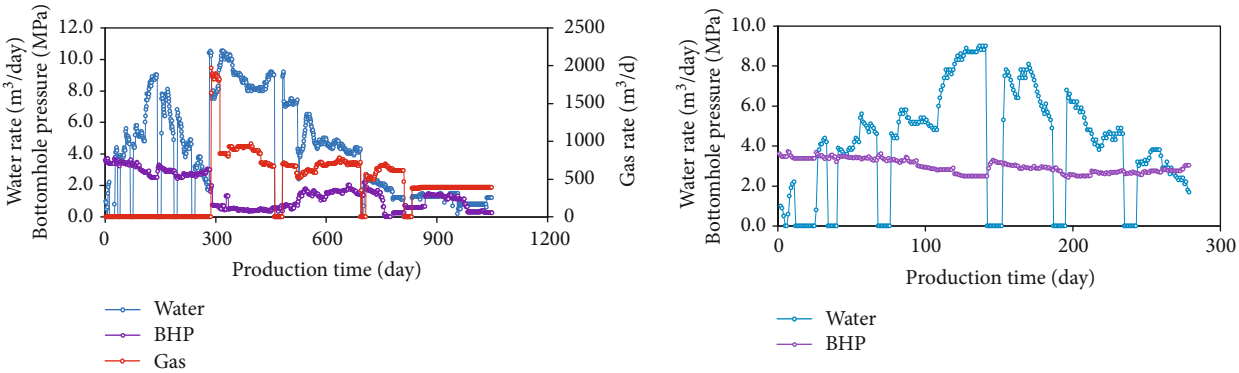

(a) Production history (b) Early dewatering stage

Figure 11: The production history of the well ZY-n (Qinshui Basin, China).

denudation are set as zero to show the production performance without considering fines migration (blue line in Figure 12).

When the simulation takes fines migration into consideration, the water rate cannot recover to the standard before the well is shut. The simulated results match well with the history data, which also agrees with the tendency in the simulation in Section 4.3. When simulation is performed without considering the fines migration (blue curve in Figure 12), the water rate is substantially higher than history data after the second well shut and the water production rate can return to the value before well shut. Because the first well shut is not caused by fines production, the difference between two simulation results is not significant. As fines migration triggers the jamming of the flow channel in the coal seam, the permeability changes and the difference between two simulations become dramatic.

5. Conclusion

In this study, the coal fines migration process can be modeled as one curve (the maximum water carrying capacity of coal fines), two states (static and flowing fines), three stages (generation, migration, and deposition), and four processes (detachment, denudation, reattachment, and blockage). New models are established to describe the fines transport in the early water drainage period of CSG reservoirs, and a practical solution is proposed to solve coal fines migration coupled with water flow. Three simulation cases and one field case were performed with the main conclusions drawn as follows:

(1) The continuous water flow leads to a low concentration of static fines (almost zero) near the wellbore, which improves the coal permeability within the wellbore neighborhood. When the water production does not decline, the new generated fines can be transported with flowing water and do not influence the production significantly

(2) The water rate decline significantly affects the coal permeability. When the fast depressurization strategy is employed, massive fines are detached and new fines are generated, which leads to temporary increase in

Table 4: Input and adjusted parameters in the simulation of the well ZY-n.

Parameter	Input value	Adjusted value
Grid size (m × m × m)	10 × 10 × 4	
Coal size (m × m × m)	400 × 400 × 4	
Cleat porosity of coal (%)	0.82	
Cleat permeability of coal (mD)	3.24	
Initial pressure of coal (MPa)	3.62	3.58
Gas content of coal (m^3/m^3)	18.45	
Langmuir volume (m^3/m^3)	38.54	
Langmuir pressure (MPa)	2.95	
Initial water saturation (%)	100	
Half-length of HF (hydraulic fracture) (m)	55	45
Conductivity* of HF (mD·m)	42	21
Compressibility of coal (10^{-4} MPa^{-1})	0.00245	0.01225
Water density (g/cm^3)	1.04	
Coal density (g/cm^3)	1.35	
Water dynamic viscosity (mPa·s)	1.14	
Initial static fines concentration (m^3/m^3)	0.0032	0.0064
Initial static fines distribution	5 grids around the well	Whole reservoir

*Conductivity is the product of permeability and facture width.

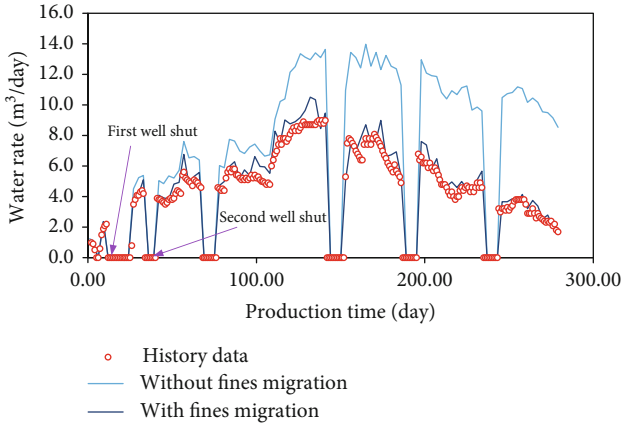

Figure 12: The history results with and without considering fines migration.

the permeability. When the water rate declines, these generated fines will clog the flow channels and bring severe damage to the coal permeability. Hence, the multiple well shuts will dramatically reduce the well productivity when the fast depressurization strategy is applied

(3) The field case study indicates that the water rate cannot recover to the initial value when the well is shut when fines migration is triggered. The simulation without considering fines migration could overestimate the productivity. Taking fines migration into account, the simulated rate can match the history data owing to the blockage of flow channels and permeability reduction induced by fines migration

(4) Although the fast depressurization strategy can improve the coal permeability at the beginning, the water rate of a CSG reservoir will always decline, which may cause fines deposition. Therefore, the moderate depressurization strategy is a more reliable way to continuously produce the fines, avoid new generated fines, and protect the coal permeability from damage induced by fines migration

Appendix

The Numerical Solution of the Coupled Flow Problem

Newton's iteration is an effective approach to solve the system of nonlinear equations. In the appendix, we take the one-dimensional flow in the coal as an example to introduce the numerical solution process.

(1) *Governing Equation for Water Flow.*

$$\left[\frac{T^{\lambda}_{wi+1/2}}{B_w}p_{w,i+1}+\frac{T^{\lambda}_{wi+1/2}}{B_w}p_{w,i-1}-\left(\frac{T^{\lambda}_{wi+1/2}}{B_{w,i}}+\frac{T^{\lambda}_{wi-1/2}}{B_{w,i}}\right)p_{w,i}\right]-\frac{V_i}{\Delta t}\left[\left(\frac{\phi}{B_w}\right)^{n+1}_i-\left(\frac{\phi}{B_w}\right)^{n}_i\right]+\left(\frac{q_w}{B_w}\right)_i=0, \tag{A.1}$$

where $T^{\lambda}_{L+1/2}=(A_{yz}K\alpha/\mu_w)^{(n)}_{i+1/2}$.

Since Equation (A.1) is a function of $p^{n+1}_{w,i+1}$, $C^{n+1}_{f,i+1}$, $C^{n+1}_{s,i+1}$, $p^{n+1}_{w,i}$, $C^{n+1}_{f,i}$, $C^{n+1}_{s,i}$, $p^{n+1}_{w,i-1}$, $C^{n+1}_{f,i-1}$, $C^{n+1}_{s,i-1}$, it can be rewritten in the form

$$F_{w,i}\left(p^{n+1}_{w,i+1},C^{n+1}_{f,i+1},C^{n+1}_{s,i+1},p^{n+1}_{w,i},C^{n+1}_{f,i},C^{n+1}_{s,i},p^{n+1}_{w,i-1},C^{n+1}_{f,i-1},C^{n+1}_{s,i-1}\right)=0. \tag{A.2}$$

(2) *Governing Equation for Fines Transport.*

The finite difference form is

$$\begin{aligned}&\varsigma^{(n)}_{vi}\left\{T_{wi+1/2}\left(p_{w,i+1}-p_{w,i}\right)-T_{wi-1/2}\left(p_{w,i}-p_{w,i-1}\right)\right\}\\&\quad-A\varsigma^{(n)}_{ci}\left(C_{f,i+1/2}-C_{f,i-1/2}\right)\\&\quad-\left(\frac{V\phi}{\rho_s}\frac{C^{n+1}_{f,i}-C^{n}_{f,i}}{\Delta t}+2c_s\phi V\frac{P^{n+1}_w-P^{n}_w}{\Delta t}\right)\\&\quad-\frac{Vm_{tr}}{\rho_s}-\frac{Vm_{pr}}{\rho_s}=0,\end{aligned} \tag{A.3}$$

where $\varsigma_{vi}^{(n)} = (\partial\omega/\partial C_f)_i^{(n)}$, $\varsigma_{Ci}^{(n)} = (\partial\omega/\partial C_f)_i^{(n)}$, and $T_w = AK/\phi\mu_w B_w \Delta x$ and Equation (A.4) is

$$F_{C_f,i}\left(p_{w,i+1}^{n+1}, C_{f,i+1}^{n+1}, C_{s,i+1}^{n+1}, p_{w,i}^{n+1}, C_{f,i}^{n+1}, C_{s,i}^{n+1}, p_{w,i-1}^{n+1}, C_{f,i-1}^{n+1}, C_{s,i-1}^{n+1}\right) = 0. \tag{A.4}$$

(3) *Mass Conservation of Static Fines.*

$$\min\left[\left(\frac{\partial C_{mxf}}{\partial v_w}\right)^{(n)}\left(\frac{K}{\mu_w}\frac{p_{w,i+1}^{n+1} - p_{w,i-1}^{n+1}}{2\Delta x} - v_{w,i}^{n}\right), C_{s,i}\right] - \left[\left(\frac{\phi C_s}{B_s}\right)_i^{n+1} - \left(\frac{\phi C_s}{B_s}\right)_i^{n}\right] = 0. \tag{A.5}$$

Thus, it is written in the form

$$F_{C_s,i}\left(p_{w,i+1}^{n+1}, C_{f,i+1}^{n+1}, C_{s,i+1}^{n+1}, p_{w,i}^{n+1}, C_{f,i}^{n+1}, C_{s,i}^{n+1}, p_{w,i-1}^{n+1}, C_{f,i-1}^{n+1}, C_{s,i-1}^{n+1}\right) = 0. \tag{A.6}$$

Because the coal fines concentration depends on the water velocity, in order to deal with the nonlinearity of the equation, the coal fines concentration and the pressure are solved using the iterative approach. At each time step, Newton's iterative method for the one-dimensional coal fines-water flow model can be described as

Step 1. k is set to zero.

Step 2. The pressure and saturation from a previous time step $t = t^n$ are taken as the initial values of the present time step.

$$p_{w,i}^{\{k\}} = p_{w,i}^{(n)}, C_{s,i}^{\{k\}} = C_{s,i}^{(n)}, C_{f,i}^{\{k\}} = C_{f,i}^{(n)} \quad (\forall i \in \{1 \cdots N\}). \tag{A.7}$$

Step 3. The system of governing equations can be expressed as

$$\begin{aligned} r_{w,i}^{\{k\}} &= F_{w,i}\left(p_{w,i+1}^{\{k\}}, C_{f,i+1}^{\{k\}}, C_{s,i+1}^{\{k\}}, p_{w,i}^{\{k\}}, C_{f,i}^{\{k\}}, C_{s,i}^{\{k\}}, p_{w,i-1}^{\{k\}}, C_{f,i-1}^{\{k\}}, C_{s,i-1}^{\{k\}}\right), \\ r_{C_s,i}^{\{k\}} &= F_{C_s,i}\left(p_{w,i+1}^{\{k\}}, C_{f,i+1}^{\{k\}}, C_{s,i+1}^{\{k\}}, p_{w,i}^{\{k\}}, C_{f,i}^{\{k\}}, C_{s,i}^{\{k\}}, p_{w,i-1}^{\{k\}}, C_{f,i-1}^{\{k\}}, C_{s,i-1}^{\{k\}}\right), \\ r_{C_f,i}^{\{k\}} &= F_{C_f,i}\left(p_{w,i+1}^{\{k\}}, C_{f,i+1}^{\{k\}}, C_{s,i+1}^{\{k\}}, p_{w,i}^{\{k\}}, C_{f,i}^{\{k\}}, C_{s,i}^{\{k\}}, p_{w,i-1}^{\{k\}}, C_{f,i-1}^{\{k\}}, C_{s,i-1}^{\{k\}}\right), \\ &(i = 1, 2 \cdots N). \end{aligned} \tag{A.8}$$

Calculate the corrections as

$$\begin{aligned} \delta p_{w,i}^{\{k\}} &= P_i^{\{k+1\}} - P_i^{\{k\}}, \delta C_{s,i}^{\{k\}} = C_{s,i}^{\{k+1\}} - C_{s,i}^{\{k\}}, \delta C_{f,i}^{\{k\}} \\ &= C_{f,i}^{\{k+1\}} - C_{f,i}^{\{k\}}. \end{aligned} \tag{A.9}$$

Step 4. Construct the Jacobian matrix as

$$\mathbf{J} = (J_1, J_2, \cdots, J_i, \cdots, J_N)^T, \tag{A.10a}$$

where

$$J_i = \frac{\partial\left(F_{w,i}, F_{C_s,1}, F_{C_s,i}\right)}{\partial\left(p_{w,i+1}, C_{f,i+1}, C_{s,i+1}, p_{w,i}, C_{f,i}, C_{s,i}, p_{w,i-1}, C_{f,i-1}, C_{s,i-1}\right)}. \tag{A.10b}$$

Solve Equations (A.10a) and (A.10b) by Newton's iteration method.

$$\begin{pmatrix} J_1^{\{k\}} \\ \\ \\ \cdots \\ J_i^{\{k\}} \\ \\ \\ \cdots \\ J_N^{\{k\}} \\ \\ \end{pmatrix} \begin{pmatrix} \delta P_{w,1}^{\{k\}} \\ \delta C_{w,1}^{\{k\}} \\ \delta C_{w,1}^{\{k\}} \\ \cdots \\ \delta P_{w,i}^{\{k\}} \\ \delta C_{w,i}^{\{k\}} \\ \delta C_{w,i}^{\{k\}} \\ \cdots \\ \delta P_{w,N}^{\{k\}} \\ \delta C_{f,N}^{\{k\}} \\ \delta C_{s,N}^{\{k\}} \end{pmatrix} = \begin{pmatrix} r_{w,1}^{\{k\}} \\ r_{C_f,1}^{\{k\}} \\ r_{C_s,1}^{\{k\}} \\ \cdots \\ r_{w,i}^{\{k\}} \\ r_{C_f,i}^{\{k\}} \\ r_{C_s,i}^{\{k\}} \\ \cdots \\ r_{w,N}^{\{k\}} \\ r_{C_f,N}^{\{k\}} \\ r_{C_s,N}^{\{k\}} \end{pmatrix}. \tag{A.11}$$

Then, $\delta P_{w,i}^{\{k\}}, \delta C_{w,i}^{\{k\}}, \delta C_{w,i}^{\{k\}} (i = 1 \cdots N)$ are obtained.

Step 5. If the modulus of $\delta P_{w,i}^{\{k\}}, \delta C_{w,i}^{\{k\}}, \delta C_{w,i}^{\{k\}} (i = 1 \cdots N)$ is smaller than the predefined error threshold, the iteration is terminated. The solutions are $p_{w,i}^{n+1} = p_{w,i}^{\{k+1\}}$, $C_{w,i}^{n+1} = C_{w,i}^{\{k+1\}}$, $C_{w,i}^{n+1} = C_{f,i}^{\{k+1\}} (\forall i \in \{1 \cdots N\})$. Otherwise, let $k = k + 1$ and go to Step 3 to continue with the iteration.

Data Availability

The data used to support the findings of this study are available from the corresponding authors upon request.

Conflicts of Interest

The authors declare that they have no conflicts of interest.

Acknowledgments

This work is supported by the Southwest Petroleum University State Key Laboratory of Oil and Gas Reservoir Geology and Exploitation, which is gratefully acknowledged. Meanwhile, the authors appreciate the financial support from Natural Science Foundation of China

(51474179) and China Major Science and Technique Project (2016ZX05066004-001).

References

[1] C. R. Clarkson and A. Salmachi, "Rate-transient analysis of an undersaturated CBM reservoir in Australia: accounting for effective permeability changes above and below desorption pressure," *Journal of Natural Gas Science and Engineering*, vol. 40, pp. 51–60, 2017.

[2] A. Salmachi, C. R. Clarkson, S. Zhu, and J. A. Barkla, "Relative permeability curve shapes in coalbed methane reservoirs," in *SPE Asia Pacific Oil and Gas Conference and Exhibition*, Brisbane, Australia, 2018.

[3] Q. Feng, J. Zhang, X. Zhang, and A. Hu, "Optimizing well placement in a coalbed methane reservoir using the particle swarm optimization algorithm," *International Journal of Coal Geology*, vol. 104, pp. 34–45, 2012.

[4] S. Zhu, A. Salmachi, and Z. Du, "Two phase rate-transient analysis of a hydraulically fractured coal seam gas well: a case study from the Ordos Basin, China," *International Journal of Coal Geology*, vol. 195, pp. 47–60, 2018.

[5] A. Keshavarz, A. Badalyan, R. Johnson Jr., and P. Bedrikovetsky, "Productivity enhancement by stimulation of natural fractures around a hydraulic fracture using micro-sized proppant placement," *Journal of Natural Gas Science and Engineering*, vol. 33, no. 33, pp. 1010–1024, 2016.

[6] A. Keshavarz, R. Sakurovs, M. Grigore, and M. Sayyafzadeh, "Effect of maceral composition and coal rank on gas diffusion in Australian coals," *International Journal of Coal Geology*, vol. 173, pp. 65–75, 2017.

[7] F. Huang, Y. Kang, L. You, X. Li, and Z. You, "Massive fines detachment induced by moving gas-water interfaces during early stage two-phase flow in coalbed methane reservoirs," *Fuel*, vol. 222, pp. 193–206, 2018.

[8] F. Huang, Y. Kang, Z. You, L. You, and C. Xu, "Critical conditions for massive fines detachment induced by single-phase flow in coalbed methane reservoirs: modeling and experiments," *Energy & Fuels*, vol. 31, no. 7, pp. 6782–6793, 2017.

[9] L. Wang, Y. Cheng, and W. Li, "Migration of metamorphic CO_2 into a coal seam: a natural analog study to assess the long-term fate of CO_2 in coal bed carbon capture, utilization, and storage projects," *Geofluids*, vol. 14, no. 4, 390 pages, 2015.

[10] C. R. Clarkson and M. Bustin, "Coalbed methane: current field-based evaluation methods," *SPE Reservoir Evaluation & Engineering*, vol. 14, no. 1, pp. 60–75, 2011.

[11] D. P. Magill, M. Ramurthy, R. Jordan, and P. D. Nguyen, "Controlling coal-fines production in massively cavitated openhole coalbed-methane wells," in *SPE Asia Pacific Oil and Gas Conference and Exhibition*, Brisbane, Queensland, Australia, 2010.

[12] H. Chan, S. Chen, and Y. Chang, "Simulation: the deposition behavior of Brownian particles in porous media by using the triangular network model," *Separation Purification Technology*, vol. 44, no. 2, pp. 103–114, 2005.

[13] X. Zhang, J. Fan, S. Wu, and D. Liu, "A novel acoustic liquid level determination method for coal seam gas wells based on autocorrelation analysis," *Energies*, vol. 10, no. 12, article 1961, 2017.

[14] X. G. Zhang, R. P. Gamage, M. S. A. Perera, and A. S. Ranathunga, "Effects of water and brine saturation on mechanical property alterations of brown coal," *Energies*, vol. 11, no. 5, article 1116, 2018.

[15] H. Li, H. C. Lau, and S. Huang, "China's coalbed methane development: a review of the challenges and opportunities in subsurface and surface engineering," *Journal of Petroleum Science & Engineering*, vol. 166, pp. 621–635, 2018.

[16] Z. Yao, D. Cao, Y. Wei, X. Li, X. Wang, and X. Zhang, "Experimental analysis on the effect of tectonically deformed coal types on fines generation characteristics," *Journal of Petroleum Science & Engineering*, vol. 146, pp. 350–359, 2016.

[17] A. Keshavarz, Y. Yang, A. Badalyan, R. Johnson, and P. Bedrikovetsky, "Laboratory-based mathematical modelling of graded proppant injection in CBM reservoirs," *International Journal of Coal Geology*, vol. 136, pp. 1–16, 2014.

[18] G. Han, K. Ling, H. Wu, F. Gao, F. Zhu, and M. Zhang, "An experimental study of coal-fines migration in coalbed-methane production wells," *Journal of Natural Gas Science and Engineering*, vol. 26, pp. 1542–1548, 2015.

[19] C. Wei, M. Zou, Y. Sun, Z. Cai, and Y. Qi, "Experimental and applied analyses of particle migration in fractures of coalbed methane reservoirs," *Journal of Natural Gas Science and Engineering*, vol. 23, pp. 399–406, 2015.

[20] T. Bai, Z. Chen, S. M. Aminossadati, Z. Pan, J. Liu, and L. Li, "Characterization of coal fines generation: a micro-scale investigation," *Journal of Natural Gas Science and Engineering*, vol. 27, no. 1, pp. 862–875, 2015.

[21] A. Joseph, L. Akubue, J. Ajienka, and A. B. Oriji, "Sanding prediction using rock mechanical properties: a parametric study," in *Nigeria Annual International Conference and Exhibition*, Lagos, Nigeria, 2012.

[22] S. Xue and Y. Yuan, "Sanding process and permeability change," *Journal of Canadian Petroleum Technology*, vol. 46, no. 4, pp. 33–39, 2007.

[23] C. Gruesbeck and R. E. Collins, "Entrainment and deposition of fine particles in porous media," *Society of Petroleum Engineers Journal*, vol. 22, no. 06, pp. 847–856, 1982.

[24] H. A. Ohen and F. Civan, "Simulation of fracturing induced formation damage and gas production," in *Paper Presented at the SPE Middle East Unconventional Gas Conference and Exhibition*, Abu Dhabi, UAE, 2012.

[25] S. Chien, "Settling velocity of irregularly shaped particles," *SPE Drilling & Completion*, vol. 9, no. 4, pp. 281–289, 1994.

[26] S. A. Bradford and N. Toride, "A stochastic model for colloid transport and deposition," *Journal of Environmental Quality*, vol. 36, no. 5, pp. 1346–1356, 2007.

[27] S. Zhu, X. Peng, Z.-M. Du et al., "Modeling of coal fine migration during CBM production in high-rank coal," *Transport in Porous Media*, vol. 118, no. 1, pp. 65–83, 2017.

[28] N. Ahfir, A. Benamar, A. Alem, and H. Q. Wang, "Influence of internal structure and medium length on transport and deposition of suspended particles: a laboratory study," *Transport in Porous Media*, vol. 76, no. 2, pp. 289–307, 2009.

[29] H. Haji, A. Saouab, and C. H. Park, "Particles deposit formation and filtering: numerical simulation in the suspension flow through a dual scale fibrous media," *Macromolecular Symposia*, vol. 340, no. 1, pp. 44–51, 2014.

[30] P. Bedrikovetsky, F. D. Siqueira, C. A. Furtado, and A. L. S. Souza, "Modified particle detachment model for colloidal transport in porous media," *Transport in Porous Media*, vol. 86, no. 2, pp. 353–383, 2011.

[31] Z. You, Y. Yang, A. Badalyan, P. Bedrikovetsky, and M. Hand, "Mathematical modelling of fines migration in geothermal reservoirs," *Geothermics*, vol. 59, pp. 123–133, 2016.

[32] Y. Yang, F. D. Siqueira, A. S. L. Vaz, Z. You, and P. Bedrikovetsky, "Slow migration of detached fine particles over rock surface in porous media," *Journal of Natural Gas Science and Engineering*, vol. 34, pp. 1159–1173, 2016.

[33] Z. You, A. Badalyan, Y. Yang, P. Bedrikovetsky, and M. Hand, "Fines migration in geothermal reservoirs: laboratory and mathematical modelling," *Geothermics*, vol. 77, pp. 344–367, 2019.

[34] M. M. Sharma, H. Chamoun, D. S. H. S. R. Sarma, and R. S. Schechter, "Factors controlling the hydrodynamic detachment of particles from surfaces," *Journal of Colloid & Interface Science*, vol. 149, no. 1, pp. 121–134, 1992.

[35] P. Sharma, M. Flury, and E. D. Mattson, "Studying colloid transport in porous media using a geocentrifuge," *Water Resources Research*, vol. 44, no. 7, 2008.

[36] N. Tufenkji, "Modeling microbial transport in porous media: traditional approaches and recent developments," *Advances in Water Resources*, vol. 30, no. 6-7, pp. 1455–1469, 2007.

[37] X. Zhao, S. Liu, S. Sang et al., "Characteristics and generation mechanisms of coal fines in coalbed methane wells in the southern Qinshui Basin, China," *Journal of Natural Gas Science and Engineering*, vol. 34, pp. 849–863, 2016.

[38] F. Civan, *Reservoir Formation Damage: Fundamentals, Modeling, Assessment, and Mitigation*, Elsevier, Gulf Professional Publishling, Burlington, Second Edition edition, 2007.

[39] F. Clark and B. Harkin, "Experimental investigation of multilayer particle deposition and resuspension between periodic steps in turbulent flows," *Journal of Aerosol Science*, vol. 64, no. 1, pp. 111–124, 2013.

[40] S. C. James and C. V. Chrysikopoulos, "Effective velocity and effective dispersion coefficient for finite-sized particles flowing in a uniform fracture," *Journal of Colloid & Interface Science*, vol. 263, no. 1, pp. 288–295, 2003.

[41] R. Chen, Y. Qin, P. Zhang, and Y. Wang, "Changes in pore structure of coal caused by CS2 treatment and its methane adsorption response," *Geofluids*, vol. 2018, Article ID 7578967, 11 pages, 2018.

[42] X. Cui, A. M. M. Bustin, and R. M. Bustin, "Measurements of gas permeability and diffusivity of tight reservoir rocks: different approaches and their applications," *Geofluids*, vol. 9, no. 3, 223 pages, 2009.

[43] H. Kumar, D. Elsworth, J. P. Mathews, and C. Marone, "Permeability evolution in sorbing media: analogies between organic-rich shale and coal," *Geofluids*, vol. 16, no. 1, 55 pages, 2016.

[44] I. D. Palmer and J. Mansoori, "How permeability depends on stress and pore pressure in coalbeds: a new model," *SPE Reservoir Evaluation and Engineering*, vol. 1, no. 06, pp. 539–544, 1998.